OVERVIEW OF OXYGEN REDUCTION CATALYST

by

Christian Nguyen

(Under the Direction of Professor Jin Xie)

ABSTRACT

Oxygen reduction catalysts are of great interest both as a source of renewable energy as well as serving biological relevance. One such example is Cytochrome C oxidase which is known to reduce O_2 into H_2O. To develop a catalyst that also does this, a deep understanding of the structure-property relationship between Cytochrome C oxidase and O_2 interaction is necessary. Such catalyst typically uses a Fe-centered porphyrin, like the case of Cytochrome C oxidase. However, much work is done in looking at the secondary coordination sphere effect for these catalysts diving into the mechanistic studies that these oxygen reduction catalysts go through. This work aims to summarize the current O_2 reduction catalyst and current advancements in the field.

INDEX WORDS: Oxygen Reduction, Catalyst, Electrochemistry

OVERVIEW OF OXYGEN REDUCTION CATALYST

by

Christian Nguyen

B.S., The University of Clemson 2018

M.S. The University of Clemson 2020

A Thesis Submitted to the Graduate Faculty of The University of Georgia in Partial Fulfillment
of the Requirements for the Degree

MASTER OF SCIENCE

ATHENS, GEORGIA

2023

OVERIVEW OF OXYGEN REDUCTION CATALYSIT

by

Christian Nguyen

Major Professor:	Jin Xie
Committee:	Jeffery Urbauer Eric Ferreira

Electronic Version Approved:

Ron Walcott
Dean of the Graduate School
The University of Georgia
August 2023

ACKNOWLEDGEMENTS

I would like to thank Jin Xie for guiding me with this thesis. I would also like to thank my committee members Jeffery Urbauer and Matthew Ferreira for their service on my committee.

TABLE OF CONTENTS

Page

Overview of Oxygen Reduction Catalyst

CHAPTER 1

INTRODUCTION

Chapter 1.1 Importance of Cytochrome C Oxidase

Oxygen reduction plays a vital role in several fields such as energy economy as well as biological importance. (1) An example in nature is cytochrome c oxidase (CCO). Since its discovery in 1977 extensive research has been done to understand the enzyme and how its process to reduce O_2 is understood. (2) Cytochrome C oxidase utilizes a heme/ Cu active site to reduce oxygen to H_2O.(3) O_2 reduction to H_2O is a 4H/4e transfer process which requires an E_o of 1.23 V Vs NHE.(4)

The mechanism of CCo is divided into 4 steps. The first is the introduction of oxygen into the active site where the Cu^+ reduces the O_2 into superoxide which allows for binding at the Fe site. Upon binding at the Fe site, a $1e^-/H^+$ process is introduced allowing for the removal 1 one water molecule while a Fe (IV) oxo is formed. The Fe (IV) oxo undergoes another $1e^-/2\ H^+$ event to release the second equivalent of H_2O. Then another e^- is introduced to reduce the Cu^{2+} back to Cu (I) so that catalysis can start again. (5) This mechanism highlights the importance of electron transfer in the CCo system. Moreover, the highlight of a Fe (IV) oxo shows the importance of being able to access several different oxidation states for the catalytic cycle.

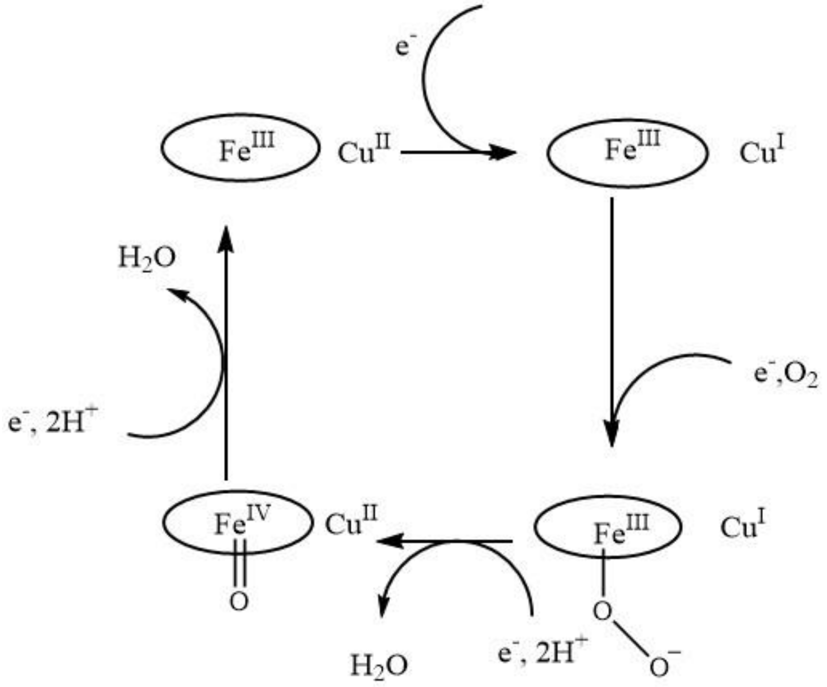

Figure 1.1 Schematic of Reduction of O_2 in CCo

Chapter 1.2 Porphyrins in Nature

In terms of ORR typical platinum or ruthenium catalysts are commonly used. However, such TM is often relatively expensive for use in terms of energy production thus a need to look at alternatives is required. An example of ORR in nature is the CCo enzyme however the framework (Fe porphyrins) is ubiquitous as a result when modeling there is an abundance of ligand frameworks to model after. Examples discovered in nature are the hemoglobin which is responsible for oxygen carried throughout mammalian species although it does not reduce oxygen it however has an affinity for binding as well as a similar ligand frame. Moreover, nature has provided several examples of Heme structures Heme c, Heme d Heme b, and Heme a. Heme a is responsible for O_2 respiration (6) while heme b is responsible for O_2 transport. (7) Heme c is the macrocyclic ring that is found in Cytochrome C.(8) Heme d is also responsible for ORR in bacterial cells. (9) This has led to showing that the macrocyclic heme structure promotes the binding of O_2 in the cases of heme a, b, and c. Moreover, oxygen binding occurs in these known biological hemes.

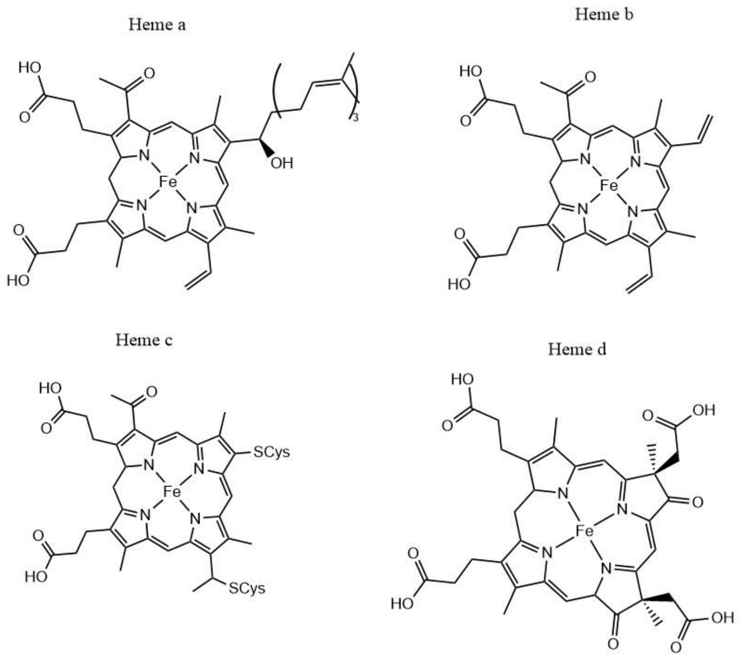

Figure 1.2 Examples of Heme found in biology.

Chapter 1.3 Figures of Merit

Typical figures of merit for accessing any kind of catalytic include the turnover number (TON), turnover frequency (TOF), and over potential. The turnover number is derived from the number of times a catalyst goes through the cycle before degradation. (10) While TOF is looking at how fast the cycle is happening and is often closely related to the catalyst rate of reaction. (11) Over potential is the difference between thermodynamic value and the potential that the catalyst undergoes catalysis.(12) Ideally when looking at catalytic design having a high TON, TOF, and a low overpotential is largely sought after. Most experiments are performed via Rotating disk electrode (RDE). An RDE consists of a 3-part electrode system a working electrode, a reference electrode, and a counter electrode. Moreover, the working electrode is spinning. This type of setup allows for monitoring reaction kinetics.

Chapter 1.4 Thermodynamics of Oxygen Reduction

As mentioned above ORR to H_2O is a $4e^-/4H^+$ transfer process. Oxygen can be reduced into two different products. The first is H_2O and the other is a $2e^-/2H^+$ proton pathway to lead to the formation of H_2O_2. Thus, a necessary understanding of thermodynamics is necessary when trying to selectively choose one product over the other. Firstly, the half-reactions are one indication of which product is favorable. O_2 to $2H_2O$ in a standard aqueous environment is 1.229 v vs SHE (Standard hydrogen electrode).(13) While the production of O_2 to H_2O_2 is 0.695 V vs SHE. (14) Moreover, the Gibbs free energy is equal to G= -zFE where Gibbs free energy G is equal to z (# of e- transferred for half-reaction) F which is the Faraday constant, and E which is the potential of the half-reaction. From this, we can approximate the Gibbs free energy and show that -237.24 kJ/mol of H_2O, while the production of H_2O_2 has about -134.1 kJ/mol. (4)

Chapter 1.5 History of ORR Complexes

As mentioned above, O_2 reduction is a $4H^+/4e^-$ transfer process in which the most used catalyst is platinum. However, since CCo utilizes Fe the uses of these metalloenzymes in biology exhibit a high affinity for O_2. Moreover, typical designs for O_2 reduction often employ Fe metal centers along with an N4 ligation system.

Proof that these types of catalysts could be made using iron porphyrins dates in 1980. Where Collman synthesized a series of tailed picket fence porphyrins. All these analogs contained a planner N4 system. Some however also contained 5-coordinate and 6-coordinate complexes. (15)

CHAPTER 2

OVERVIEW of OXYGEN REDUCTION COMPLEXES

Chapter 2.1 CCo model complexes

A notable example of an accurate CCo model was by Collman in 2009. Where a di-nuclear Fe-Cu was shown to almost reduce O_2 exclusively to H_2O. Although the rate was pH dependent the rates from 6-7 pH was about 1.8 x10^3 $M^{-1}s^{-1}$. Moreover, the experiment was conducted on the catalyst by using Cytc which is a biological reductant. Furthermore, the authors proposed a possible mechanism for O_2 reduction. Firstly, they propose that the O_2 binds to the Fe center which then gets oxidized into Fe (III). Afterwards, the Cu(I) is oxidized to Cu (II)along with the introduction of a H+ to form a Fe (IV)-oxo after which $2H^+$ /$1e^-$ is introduced from ctyc(II) to produce a Fe(III)-hydroxo then the hydroxo is protonated to form and release water. (16)

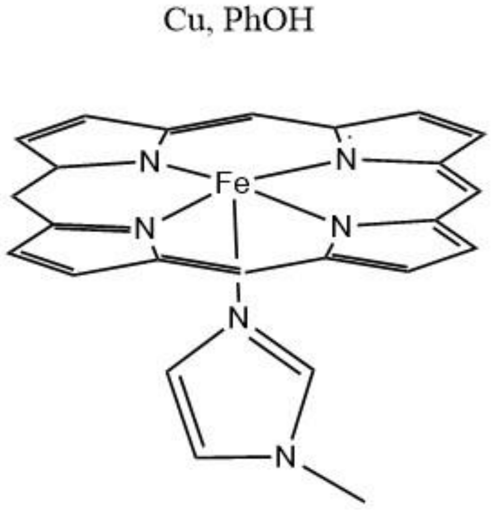

Figure 2.1: Example of axial ligand binding in an Fe porphyrin

Chapter 2.2 Iron macrocycles ORR catalyst

In more recent year's advancements have been made in terms of characterizing the effectiveness of the ORR reduction catalyst. The most notable framework for ORR reduction is the aryl Fe porphyrins. Much work is done on the Fe tetra-aryl porphyrins (figure 2.1). This complex is shown to reduce O_2 to H_2O in DMF with the detection of less than 15% H_2O_2. Moreover, the rate at which reduction occurs is measured to be around $1.1x10^6$ M^{-2} s^{-1}.

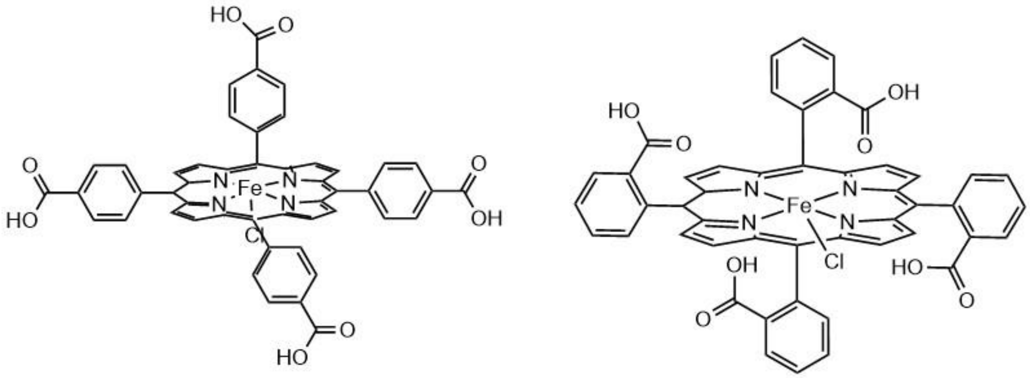

Figure 2.2 Tetra-aryl carboxylic acid groups bound to Fe porphyrin.

Moreover, the Meyer complex exhibits proton relays as aryl carboxylic acid groups. In terms of efficiency, the complex was able to obtain a TOF of 200 s^{-1} at negative 0.4 V. done using a rotating disk electrode RDE in MeCN. Following the discovery of the use of carboxylic acid groups for proton relays. (17) The Meyer group introduced pyridine groups instead of aryl carboxylic acid groups. (18) From this modification the turnover obtained went from about 200 s^{-1} to about 600 s^{-1}. These results exhibit that the use of proton relays has a dramatic effect on the ability to reduce oxygen to H_2O. Advancing on this work the introduction work done by Chlisttunoff showed that increasing the electron-donating ability of the axial ligand allowed more reactivity towards O_2.

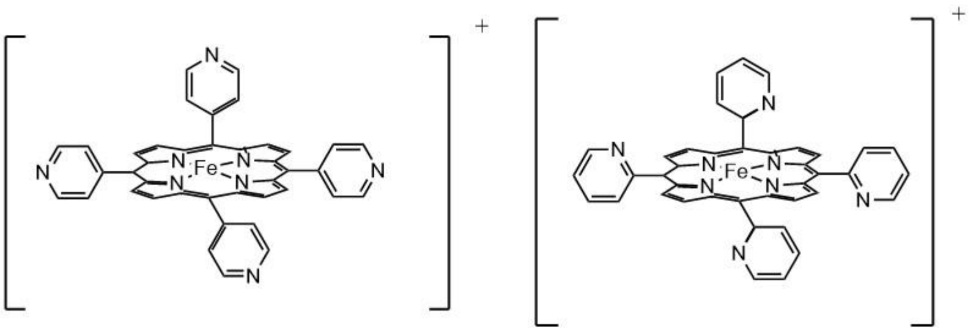

Figure 2.3 Pyridine R groups bound to Fe porphyrin ring.

Chapter 2.3 Iron Macrocycles in aqueous media

Other advancements in aqueous media are also important. Such iron systems are not necessarily porphyrin rings but contain a similar structure comprised of an N4-ligated system. Work done by Kuwana led this by designing -tetrakis(N-methyl pyridyl) porphyrins. (19) As shown in Figure 2.3. Here they show modifications of the R groups as pyridium modifications. (18) However, such a ligand framework has two competing reactions, one where O_2 goes to H_2O_2 or H_2O. Although the exact TOF was never fully calculated. In other work Matson and coworkers displayed that the non-Pyridium analogs were more selective for H_2O than H_2O and thus more prone to go through the $4e^-/4H^+$ pathway.

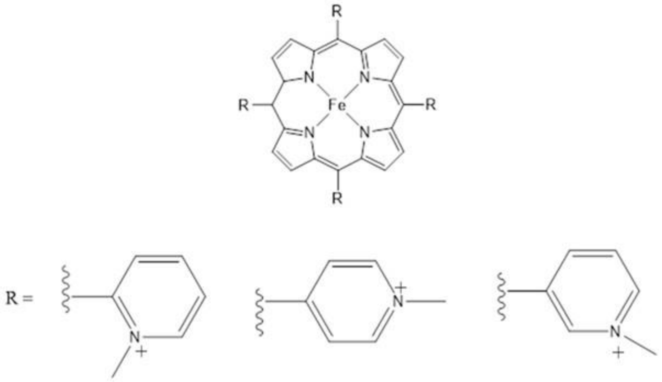

Figure 2.4 Methyl-Pyridium R groups bound to Fe porphyrin ring (4)

Chapter 2.4 Non-Fe ORR catalyst

Similarly, cobalt (II) macrocycles are also studied for O_2 reduction. In many similar ways, cobalt has a high affinity for O_2 as well. However, such models show only to have a major product of H_2O_2 instead of H_2O. Such examples are mononuclear Co Corrole complexes. Moreover, cobalt-based ORR catalyst involves a much more complex di-facial structure. Porphyrins and corroles are still typically utilized; however, two porphyrins' rings are linked together to help influence O_2 binding. The proposed mechanism allows for the binding of superoxide. Oxidizing one of the cobalt (II) into Co (III) thus facilitating O-O bond cleavage. This produces a Co-oxyl radical and portioning each bound oxygen twice to form two units of H_2O. The addition of a di-nuclear species in cobalt two helps allow for full reduction of O_2 to H_2O.(4)

Another metal that has been used to show perform O_2 reduction is the use of Mn. One such example of this was done by the Norcea group and the use of the hangman porphyrins. The idea was that the use of the axial pendant on the Mn porphyrin ring will allow for disruption of the O-O bond and make the bond easier the cleave. For this study, they took MnTPP as well as Mn(HPX-Co_2H) or Mn(HPX-CO_2Me)(figure 2.5). The study highlighted the importance of the formation of the hydroyperoxo intermediate step that is most likely to allow for the formation of H_2O. (20)

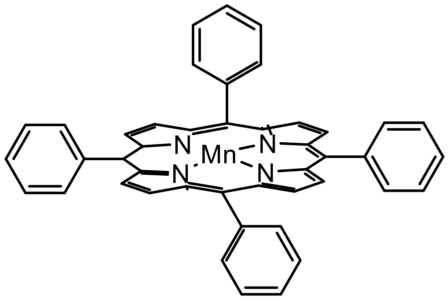

MnTPP

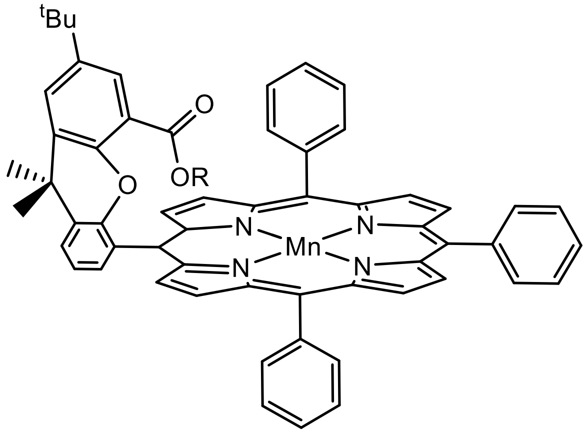

Mn(HPX-CO_2H): R=H
Mn(HPX-CO_2Me): R = CH_3

Figure 2.5 Examples of Mn catalyst

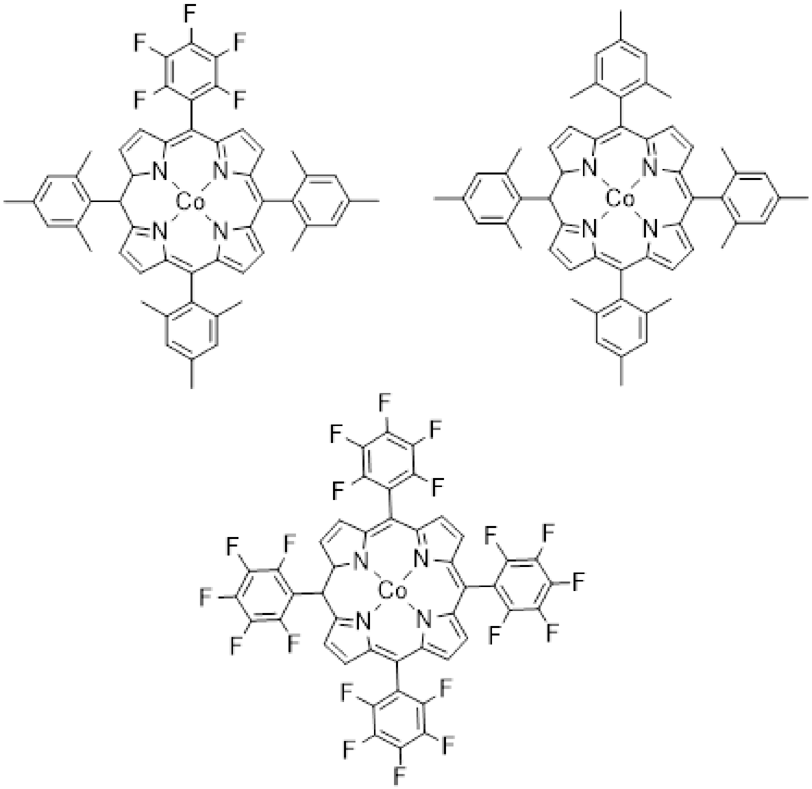

Figure 2.6 Example of Cobalt Corroles ORR catalyst (4)

Chapter 2.5 Non-heme ORR Complexes

Despite many ORR catalysts being macrocyclic, there are examples of ORR catalysts being non-heme. Such an example is the iron complex developed by Soo and coworkers in 2009. Where they discovered evidence that the N4Py platform could be used to reduce O_2 by O-O bond activation, cleavage, and then followed by electron couple proton transfer.

Moreover, typical non-heme ORR complexes tend to utilize Mn as opposed to Fe as a model. Some of the 1st notable frameworks for this were the catechol ligand framework. However, this catalyst seemed to only promote $2e^-/2H^+$ transfer thus the major product was typically H_2O_2.(4)

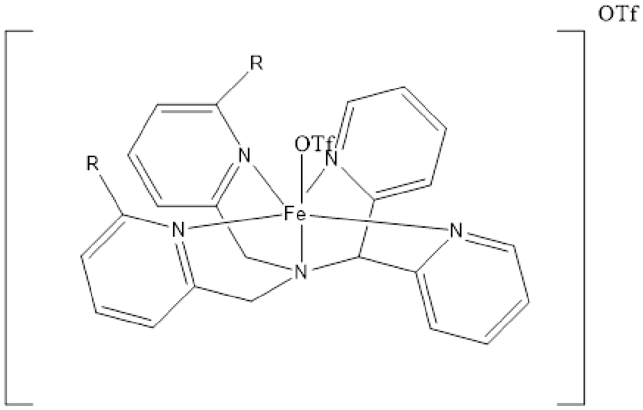

R= NHPh, NHNp, H

Figure 2.7 Example of Non-Heme Fe ORR catalyst (4)

Chapter 2.6 Summary and comparison of ORR catalyst

Incomparison of all the ORR catalysts discussed, there are some notable similarities and differences. Firstly, the major similarity is that all these ORR catalysts utilize nitrogen donor sets regardless of whether the complex is non-heme or heme, or the metal used. Next, the Fe complex typically uses heme ligand framework with modification of that frame for 2nd coordination sphere effects. However, having a heme framework is not necessarily a requirement for ORR catalysis. Below is a table summarizing all the ORR catalysts discussed in chapter two.

Catalyst	Metal center	Ligand frame	Primary product (H_2O_2 or O_2)
Iron(III)*meso*-tetra(2 carboxyphenyl)porphine chloride	Fe	Porphyrin Ring	About 9% of H_2O_2 detected
Fe(III)-meso-tetra(pyridyl)porphyrins	Fe	Porphrin	5-11 % H_2O_2
Fe(III)TMPyP	Fe	Porphyrin	NA
(5,10,15-tris(pentafluorophenyl)corrole)cobalt (TPFCor)Co	Co	Corrole	H_2O_2
10-pentafluorophenyl-5,15-dimesitylcorrole)cobalt (F5PhMes2Cor)Co	Co	Corrole	H_2O_2
(5,10,15-trismesitylcorrole)cobalt	Co	Corrole	H_2O_2
MnTPP	Mn	Porphyrin	H_2O
Mn(HPX-CO2H)	Mn	Porphyrin	H_2O
Mn(HPX-CO2Me)	Mn	Porphyrin	H_2O
FeN4Py	Fe	N4Py	H_2O

Overview of Oxygen Reduction Catalyst

CHAPTER 3

Molecular modeling

Chapter 3.1 Comparison of ORR Catalyst to CCo

From the examples described throughout Chapter 2 each ORR complex bears significant similarities to CCo, either in terms of ligand design or incorporating iron as a metal. When looking at CCo one can see that the metal center is Fe followed by a redox-active ligand frame (the porphyrin ring) as well as a histidine residue in the axial position. The ORR complexes mentioned in chapter 2 incorporate a corrole ligand sphere such as the case with the cobalt complexes. The corrole framework is another redox ligand frame, this suggests that a redox-active ligand frame is essential in ORR design likely because it can help facilitate electron transfer and stabilize certain intermediates in the catalytic cycle. Corrole and porphyrin ligand framework contain an N4 donor set which is an electron-donating group that could help facilitate stability in the change in oxidation states. For example, when looking at all the metals used in these systems Co, Mn, and Fe all can cycle through a variety of oxidation states for iron it goes from a Fe (II/III) couple and perhaps and Fe (IV)-oxo intermediate. While Co (II/III) couple and the Mn are proposed to go through Mn (II/III) couple as well as proposed to go through an Mn(V)-oxo intermediate. This heavily implies that for the design of an ORR catalyst, there needs to be access to several redox states for the binding and activation of O_2 to form either H_2O_2 or H_2O. When looking at the proposed mechanism for CCo one can see why these metals and ligand framework were picked specifically for ORR catalysis.

Chapter 3.1 O_2 Binding Modes

To discuss structure-activity relationships firstly O_2 binding modes need to be discussed. Binding modes of ORR complexes typically just consider the binding of oxygen at the metal site. For a mononuclear species, there are two types of bonding modes and for a di-nuclear catalyst, there are also two bonding modes. Firstly, the monocular nuclear species can bind as a η_1-superoxide giving a bent geometry to the superoxide. The other option is a η_2-peroxo where the binding forms a three-membered ring. In the case of di-nuclear catalyst, there exist only the cis and trans binding modes (figure 3.1). (4)

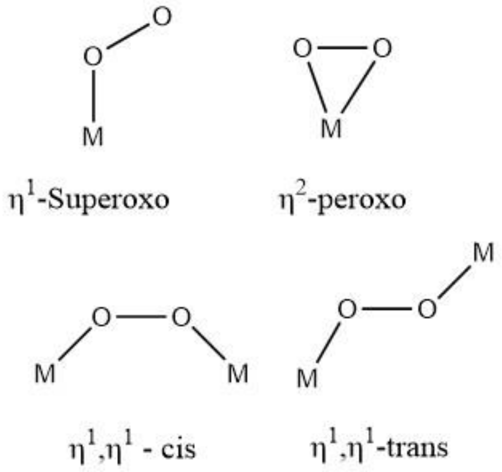

η^1-Superoxo η^2-peroxo

η^1,η^1 - cis η^1,η^1-trans

Figure 3.1 Binding modes of oxygen to metal site

Chapter 3.2 Mechanism of ORR Catalyst

Typically, the proposed mechanism of these ORR catalysts follows what is done with CCo. However, it is possible to end up with partially reactive oxygen species (H_2O_2). In a similar fashion O_2 starts the binding mode to the Fe (II) center typically in a η_1 oxo unit before an internal electron transfer to make the superoxo and oxidize the Fe (II) to Fe (III). Afterward the Fe (III)-superoxide species can either be protonated to release H_2O_2 or promote electron-coupled proton transfer hereby releasing H_2O and forming a Fe (IV)-oxo intermediate which undergoes another PCET process to release another unit of H_2O.(21, 22)

Chapter 3.3 Primary Coordination Spheres

From these examples of ORR catalysts mentioned in Chapter 2, there are certain similarities between all these models. That is that they typically incorporate a Fe or Co metal center. This likely has to do with the binding affinity for O_2 with these two species. Fe (II) and Co (II) have high reactivity due to the octahedral configuration of the complexes. More specifically, Co (II) and Fe (II) are high spins thus they are reactive in the D_z^2 orbital resulting in effective binding of O_2. However, as mentioned above Co ORR complexes typically stop at the $2e^-/2H^+$ transfer process. While Fe can facilitate a $4e^-/4H^+$ transfer process. This is likely because Co is beyond the oxo wall. As mentioned before a Fe (IV)-oxo is a proposed intermediate for the complete reduction to H_2O. The oxo-wall is a theory that metal-oxo species cannot exist past a d^5 configuration. The reason for this is that as electrons are added to the orbitals the bond order gradually decreases. For example, the Fe (IV)-oxo consists of 5 electrons and thus the bond order for the oxo is 2. Bond order is calculated by the number of bonding electrons – the number of bonds in the anti-bonding orbital. (23) The formation of this metal-oxo bond increases stability and allows for further PCET. (4)

Chapter 3.4 2nd Coordination Sphere Effects

Efforts to utilize 2nd coordination sphere effects were employed to help influence catalytic rates and O_2 binding affinity. The Dey group further synthesized a multi-nuclear complex to symbolize the enzyme more closely by the utilization of ferrocene groups. The ferrocene acts as an electron transfer site and thus promotes could potentially affect the electron transfer rate to the metal center. It hopes that this modification will allow for the $4e^-/4H^+$ transfer process as opposed to the formation of H_2O_2 which is a $2e^-/2H^+$ process.

Firstly, they synthesized 3 different analogues that incorporated 4 ferrocene units, one just consisted of 4 ES4 groups, and one consisted of 1 Fc group and 3 ES3 groups. The results indicated that the analog with 4 ferrocenes consisted of the production of 11.5 % of H_2O_2 while the no ferrocene analog consisted of nearly 100 % H_2O_2. Then the last analog produced nearly 42% of H_2O_2. This suggests that the 2nd coordination sphere modification has a dramatic effect on the selectivity of H_2O over H_2O_2. It almost seems to indicate that promoting more efficient electron transfer pathways will allow the formation of H_2O. (24)

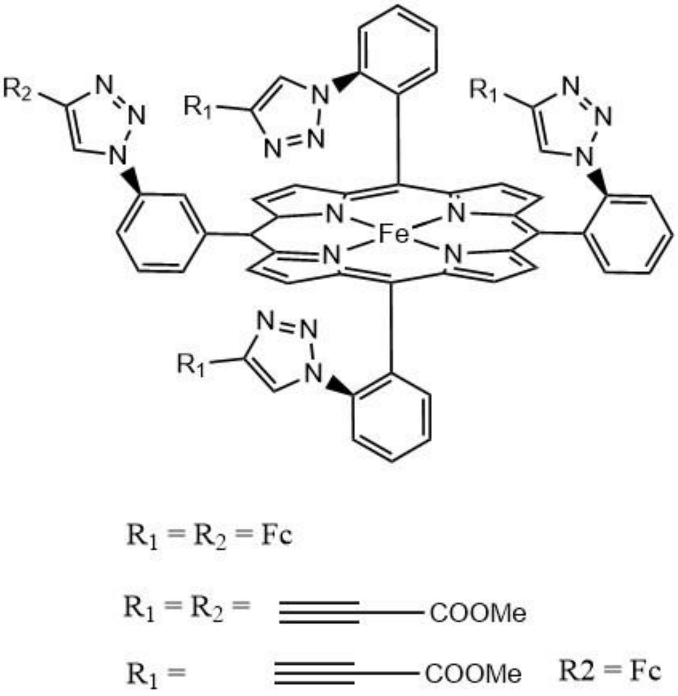

Figure 3.2 Ferrocenium R groups modified Fe porphyrin ring.

The information was collected through various spectroscopies as well as electrochemical analysis. Firstly, in the electrochemical analysis, in the CV the analogues that contained Fc analogues show a Fc/Fc$^+$ reversible wave. When compared to the control of Fc/Fc$^+$ there was no shift in the oxidation or reduction waves indicating the Fc R groups behaved independently of the overall molecule. Moreover, all analogs showed 2 other oxidation and reduction peaks which have been assigned as the porphyrin ring and the oxidation of the metal. To confirm O_2 binding the addition of O_2 was done by anhydrous condition. Moreover, a xylenol orange assay to detect the amount of H_2O_2. Figure 3.3 shows the binding effect of O_2 and the UV absorption spectrum. The blue trace shows the di-oxygenated adduct. While the red trace shows the reduced species, and the black trace shows the oxidized species. From the graph one can tell that the oxidized and dioxygen adducts are very similar in the UV-vis spectrum. This indicated that once O_2 binds the Fe potentially goes into a Fe (III) state.

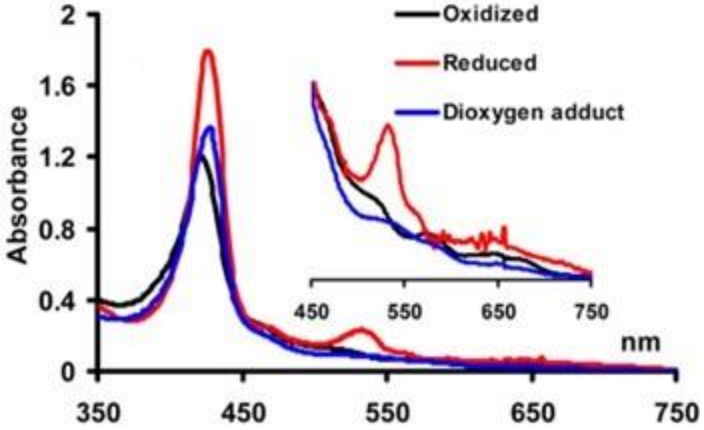

Figure 3.3 Example of O_2 binding features in UV-Vis

Chapter 3.5 Push effect by axial ligands

Work has also been done to look at the effects of axial donating ligands. Looking at a CCo there is a histidine residue in the axial position. The axial ligand also plays a role in just the reduction of O_2 to H_2O_2 and this is because there is a failure to construct a molecular that is capable to help facilitate O-O bond cleavage. Electron donating ligands help stable the Fe (IV)-oxo unit. The use of an electron-donating ligand provides electron density to the metal center. This allows electron density to the anti-bonding orbitals of the O-O bond thus weakening the bond and facilitating O-O bond cleavage. (25, 26) This allows ways to turn the catalytic rate as well as the selectivity of either H_2O_2.

The push effect showing influence over rate is well illustrated in Dey's work in 2013. Here a porphyrin ring was modified with benzyl rings along with having a thiolate donating group. The results indicated a rate of 5.6×10^6 $M^{-1}s^{-1}$. Other analogs having a phenolate and an imidazole group were also indicated. The rate of these analogues showed that the phenolate had a rate of 3.8×10^5 M^{-1} s^{-1}. The imidazole had a rate of 5×10^4 M^{-1} s^{-1}. These results show that the more electron donating group allows for an increase in catalytic rate. (27)

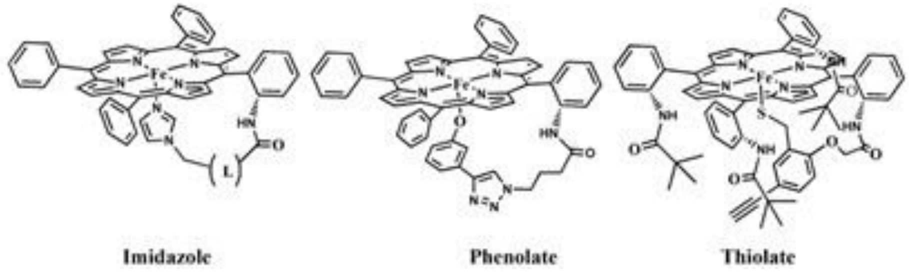

Figure 3.4 Examples of modifying axial ligands via push effect

Chapter 3.6 Pull Effect

Like the push effect, one can design a catalyst with the pull effect in mind. The pull effect is the use of hydrogen bonding to help weaken the O-O bond prompting it for cleavage. As shown in Figure 3.4 (28) Such work is also done by the Dey group in 2018 where a dramatic rate increase was obtained by having an overhanging amine pendant on their Fe porphyrin ring that was allowed to engage in H bonding with the O_2. This modification produced > 90% of H_2O while a have a rate that was about 10^7 M^{-1} s^{-1}.

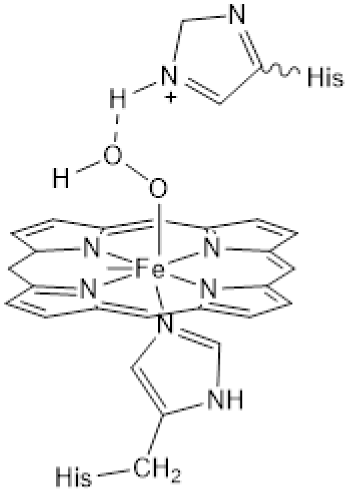

Figure 3.5 Example of how push effect interacts to promote O-O bond cleavage.

Chapter 3.7 Selectivity of H_2O over H_2O_2

Typically, the production of H_2O_2 is considered unfavorable and the most desired product is H_2O. The determination of the formation of H_2O_2 or H_2O is dictated by the pK_a of the bound O_2 species which is largely dictated by the push effect. In order words the ability of the O-O bond to be protonated affects which pathway to undergo. If the M-OOH intermediate is basic enough it will result in cleave of the O-O bond rather than protonate and form H_2O_2. Such work was conducted by the Dey group in 2014 by evaluating the pK_a of heme analogs containing different axial ligands and then looking at what was more likely to undergo the proposed Fe (IV)-oxo intermediate. (29)

Moreover, the pull effect described in Chapter 3.6 can also play a significant role in selectivity just as the pull effect elongates the O-O bond so does the pull effect by engaging the O-O bond in hydrogen bonding. This helps bond cleavage and thus they can go through the proposed Fe (IV)-oxo intermediate. Once the Fe (IV)-oxo is formed the oxo can then undergo $2e^-/2H^+$ transfer to form H_2O. As opposed to not cleaving the bond and allowing the M-OOH to be protonated again for H_2O_2. This push-pull effect can help promote the effective selectivity of H_2O over H_2O_2 as well as having effective electron transfer to help promote the transfer of electrons to the metal site thus improving H_2O selectivity over H_2O_2 formation.

Overview of Oxygen Reduction Catalyst

CHAPTER 4

Continued Development and Applications

As mentioned in chapter one renewable energy fuel is one of the potential applications for the potential use of these catalysts. One such example of renewable energy is fuel cell development. Typically fuel cells work by utilizing oxygen reduction to H_2O followed by an OER reaction to produce H_2 gas that is then fed into a fuel cell to produce electricity. An illustration of the feedback loop is displayed in Figure 4.1. As shown, there are 2 parts the fuel cell and the water-splitting cell. As shown the fuel cell is responsible for the production of electricity but after the electrical current is made O_2 is then inserted into the cycle to undergo oxygen reduction with the protons to produce H_2O. Which can be easily stored or fed into a water-splitting cell to produce H_2 gas for the fuel cell. As mentioned above, currently the only catalyst that is effective for this is platinum-containing. However, the cost of these rare earth metals causes a need to explore first-row transition metals.

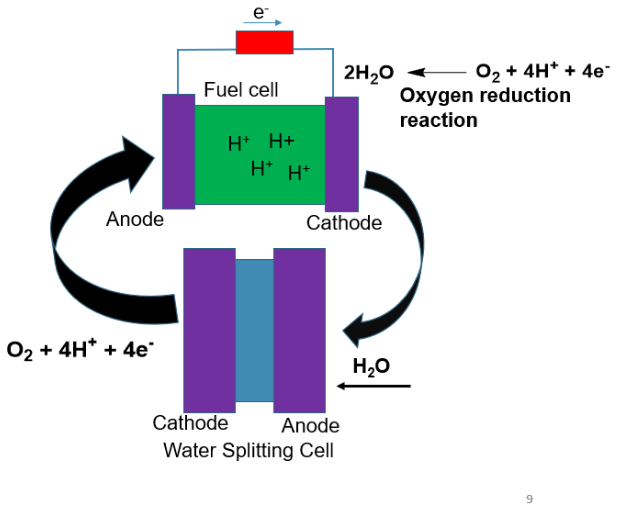

Figure 4.1 Example of Fuel cell feedback loop using ORR Catalyst

The essential challenges in ORR catalysts is the scale-up design needed for the use of fuel cells. As well as the PROS that also occur from the catalyst. The formation of H_2O_2 hinders the performance of the fuel cell application. (30) Moreover most development in the fuel cell area has been the use of carbon-supported platinum. This, however, is costly as well as the low availability of platinum. Moreover, these catalysts typically have high overpotentials. (4)

CHAPTER 5

Conclusions

In summary, looking to nature to develop an ORR catalyst leads to the use of Fe porphyrins as the most promising. As shown nature has provided a system that works well in the binding and activation of oxygen because these catalysts were developed to achieve similar efficiency. Moreover, other metals have been investigated such as the use of cobalt. These complexes typically lead to either higher PROS or just only exclusivity producing H_2O_2 instead of water due to it being beyond the oxo-wall. Moreover, the use of 2nd coordination spheres helps influence the O_2 reduction rate due to the use of proton relays and this helps mimic the CCo enzyme environment. Also, the use of the 2nd coordination sphere can be used to help pick between the production of H_2O_2 and H_2O using pendants that help facilitate proton transfer. In addition to the 2nd coordination sphere effects the axial ligands play a role in both catalytic rate as well as the selectivity of H_2O_2 or H_2O. This modification shows an increase in selectivity by utilizing electron-donating groups. The increased electron density to the metal center helps with providing electron density to the anti-bonding orbitals in the O-O bond thus weakening the bond and allowing for cleavage. Moreover, the axial ligands play a role in the catalytic rate. As shown in the Dey 2013 paper by increasing the electron-donating ability of the axial group you can also achieve high catalytic rates thus improving the performance of the ORR complex.

Nature has provided a capable platform for O_2 binding and activation, which could have promising potential to be used for renewable energy and fuel cell technologies by giving an easily accessible way to reduce O2 to water for energy storage. This could potentially lower costs and make such renewable energies more technologically accessible. Further research is required to help make ORR catalysts more efficient and limit the number of side products formed such as H_2O_2.

References

1. Dey S, Mondal B, Chatterjee S, Rana A, Amanullah SK, Dey A. Molecular electrocatalysts for the oxygen reduction reaction. *Nature Reviews Chemistry.* 2017; 1(12): 0098.

2. Wikström M, Verkhovsky MI, Hummer G. Water-gated mechanism of proton translocation by cytochrome c oxidase. *Biochimica et Biophysica Acta (BBA)-Bioenergetics.* 2003; 1604(2): 61-65.

3. Solomon EI, Stahl SS. Introduction: Oxygen reduction and activation in catalysis. *Chem Rev.* 2018; 118(5): 2299-2301.

4. Pegis ML, Wise CF, Martin DJ, Mayer JM. Oxygen reduction by homogeneous molecular catalysts and electrocatalysts. *Chem Rev.* 2018; 118(5): 2340-2391.

5. Michel H. Cytochrome c oxidase: Catalytic cycle and mechanisms of proton pumping-a discussion. *Biochemistry.* 1999; 38(46): 15129-15140.

6. Hederstedt L. Heme A biosynthesis. *Biochimica et Biophysica Acta (BBA)-Bioenergetics.* 2012; 1817(6): 920-927.

7. Louropoulou E, Gledhill M, Achterberg EP, Browning TJ, Honey DJ, Schmitz RA, Tagliabue A. Heme b distributions through the atlantic ocean: Evidence for "anemic" phytoplankton populations. *Scientific Reports.* 2020; 10(1): 4551.

8. Bowman SE, Bren KL. The chemistry and biochemistry of heme c: Functional bases for covalent attachment. *Nat Prod Rep.* 2008; 25(6): 1118-1130.

9. Bali S, Palmer DJ, Schroeder S, Ferguson SJ, Warren MJ. Recent advances in the biosynthesis of modified tetrapyrroles: The discovery of an alternative pathway for the formation of heme and heme d 1. *Cellular and molecular life sciences.* 2014; 71: 2837-2863.

10. Kozuch S, Martin JM. "Turning over" definitions in catalytic cycles. *Acs Catalysis.* 2012; 2(12): 2787-2794.

11. Rountree ES, McCarthy BD, Eisenhart TT, Dempsey JL. Evaluation of homogeneous electrocatalysts by cyclic voltammetry. *Inorg Chem.* 2014; 53(19): 9983-10002.

12. Appel AM, Helm ML. Determining the overpotential for a molecular electrocatalyst. *Acs Catalysis.* 2014; 4(2): 630-633.

13. Pegis ML, Roberts JA, Wasylenko DJ, Mader EA, Appel AM, Mayer JM. Standard reduction potentials for oxygen and carbon dioxide couples in acetonitrile and N, N-dimethylformamide. *Inorg Chem.* 2015; 54(24): 11883-11888.

14. Bockris J, Oldfield LF. The oxidation-reduction reactions of hydrogen peroxide at inert metal electrodes and mercury cathodes. *Transactions of the Faraday Society.* 1955; 51: 249-259.

15. Collman JP, Brauman JI, Doxsee KM, Halbert TR, Bunnenberg E, Linder RE, LaMar GN, Del Gaudio J, Lang G, Spartalian Kd. Synthesis and characterization of" tailed picket fence" porphyrins. *J Am Chem Soc.* 1980; 102(12): 4182-4192.

16. Collman JP, Ghosh S, Dey A, Decréau RA, Yang Y. Catalytic reduction of O2 by cytochrome c using a synthetic model of cytochrome c oxidase. *J Am Chem Soc.* 2009; 131(14): 5034-5035.

17. Carver CT, Matson BD, Mayer JM. Electrocatalytic oxygen reduction by iron tetra-arylporphyrins bearing pendant proton relays. *J Am Chem Soc.* 2012; 134(12): 5444-5447.

18. Matson BD, Carver CT, Von Ruden A, Yang JY, Raugei S, Mayer JM. Distant protonated pyridine groups in water-soluble iron porphyrin electrocatalysts promote selective oxygen reduction to water. *Chemical Communications.* 2012; 48(90): 11100-11102.

19. Kuwana T, Fujihira M, Sunakawa K, Osa T. Catalytic electroreduction of molecular oxygen using water soluble iron porphyrin. *Journal of Electroanalytical Chemistry and Interfacial Electrochemistry.* 1978; 88(2): 299-303.

20. Passard G, Dogutan DK, Qiu M, Costentin C, Nocera DG. Oxygen reduction reaction promoted by manganese porphyrins. *ACS Catalysis.* 2018; 8(9): 8671-8679.

21. Sengupta K, Chatterjee S, Samanta S, Dey A. Direct observation of intermediates formed during steady-state electrocatalytic O2 reduction by iron porphyrins. *Proceedings of the National Academy of Sciences.* 2013; 110(21): 8431-8436.

22. Chen J, Draksharapu A, Angelone D, Unjaroen D, Padamati SK, Hage R, Swart M, Duboc C, Browne WR. H2O2 oxidation by FeIII–OOH intermediates and its effect on catalytic efficiency. *ACS catalysis.* 2018; 8(10): 9665-9674.

23. Gray HB, Winkler JR. Living with oxygen. *Acc Chem Res.* 2018; 51(8): 1850-1857.

24. Samanta S, Mittra K, Sengupta K, Chatterjee S, Dey A. Second sphere control of redox catalysis: Selective reduction of O2 to O2–or H2O by an iron porphyrin catalyst. *Inorg Chem.* 2013; 52(3): 1443-1453.

25. Yan W, Xing Q, Guo O, Feng H, Liu H, Deshlahra P, Li X, Chen Y. A combination of “Push effect” strategy with “Triple-phase-boundary engineering” on iron porphyrin-based MOFs: Enhanced selectivity and activity for oxygen reduction. *ACS Applied Materials & Interfaces.* 2022; 14(45): 50751-50761.

26. Samanta S, Das PK, Chatterjee S, Sengupta K, Mondal B, Dey A. O2 reduction reaction by biologically relevant anionic ligand bound iron porphyrin complexes. *Inorg Chem*. 2013; 52(22): 12963-12971.

27. Samanta S, Das PK, Chatterjee S, Sengupta K, Mondal B, Dey A. O2 reduction reaction by biologically relevant anionic ligand bound iron porphyrin complexes. *Inorg Chem*. 2013; 52(22): 12963-12971.

28. Mukherjee S, Nayek A, Bhunia S, Dey SG, Dey A. A single iron porphyrin shows pH dependent switch between “Push” and “Pull” effects in electrochemical oxygen reduction. *Inorg Chem*. 2020; 59(19): 14564-14576.

29. Mukherjee S, Bandyopadhyay S, Chatterjee S, Dey A. Electrocatalytic O 2 reduction by a monolayer of hemin: The role of p K a of distal and proximal oxygen of a fe III–OOH species in determining reactivity. *Chemical Communications.* 2014; 50(82): 12304-12307.

30. Zaman S, Huang L, Douka AI, Yang H, You B, Xia BY. Oxygen reduction electrocatalysts toward practical fuel cells: Progress and perspectives. *Angewandte Chemie.* 2021; 133(33): 17976-17996.